



OPEN ACCESS

EDITED BY

Ingo Dreyer,
University of Talca, Chile
De Reffye Philippe,
UMR-Botanique et Modélisation de
l'Architecture des Plantes et des
végétations (AMAP), France

REVIEWED BY

Yuntao Ma,
China Agricultural University, China
Didier Combes,
L'alimentation et L'environnement (INRAE),
France
Inigo Auzmendi,
The University of Queensland, Australia

*CORRESPONDENCE

Weiwei Yang
✉ yangww@shzu.edu.cn

SPECIALTY SECTION

This article was submitted to
Plant Biophysics and Modeling,
a section of the journal
Frontiers in Plant Science

RECEIVED 06 December 2022

ACCEPTED 20 March 2023

PUBLISHED 14 April 2023

CITATION

Zhang X, Yang W, Tahir MM, Chen X,
Saudreau M, Zhang D and Costes E (2023)
Contributions of leaf distribution and leaf
functions to photosynthesis and water-use
efficiency from leaf to canopy in apple: A
comparison of interstocks and cultivars.
Front. Plant Sci. 14:1117051.
doi: 10.3389/fpls.2023.1117051

COPYRIGHT

© 2023 Zhang, Yang, Tahir, Chen, Saudreau,
Zhang and Costes. This is an open-access
article distributed under the terms of the
[Creative Commons Attribution License
\(CC BY\)](https://creativecommons.org/licenses/by/4.0/). The use, distribution or
reproduction in other forums is permitted,
provided the original author(s) and the
copyright owner(s) are credited and that
the original publication in this journal is
cited, in accordance with accepted
academic practice. No use, distribution or
reproduction is permitted which does not
comply with these terms.

Contributions of leaf distribution and leaf functions to photosynthesis and water-use efficiency from leaf to canopy in apple: A comparison of interstocks and cultivars

Xiaoyun Zhang¹, Weiwei Yang^{1*}, Muhammad Mobeen Tahir²,
Xilong Chen², Marc Saudreau³, Dong Zhang²
and Evelyne Costes⁴

¹College of Agriculture, The Key Laboratory of Special Fruits and Vegetables Cultivation Physiology and Germplasm Resources Utilization in Xinjiang Production and Construction Group, Shihezi University, Shihezi, Xinjiang, China, ²College of Horticulture, Northwest A&F University, Yangling, Shaanxi, China, ³Université Clermont Auvergne, INRAE, PIAF, Clermont-Ferrand, France, ⁴UMR AGAP Institute, University of Montpellier, INRAE, Institut Agro, CIRAD, Equipe 'Architecture et Floraison des Espèces Fruitières', Montpellier, France

Grafting has been widely used in horticulture to induce dwarfing and avoid stress-derived limitations on plant growth and yield by affecting plant architecture and leaf functions. However, the respective effects on plant photosynthesis and water use efficiency (*WUE*) of leaf distribution and functions that depend on both rootstock and scion have not been fully elucidated. This study aimed to (i) clarify the scion × interstock impacts on the variability of leaf photosynthetic traits and *WUE*, and (ii) decipher the respective effects of leaf distribution and functions on canopy photosynthesis and *WUE* (*WUE_c*). Leaf gas exchange over light gradients and responses to light, CO₂, temperature, and vapor pressure deficit were measured in two apple cultivars, 'Liquan Fuji' ('Fuji') and 'Regal Gala' ('Gala'), grafted onto rootstocks combined with interstocks: a vigorous (VV, 'Qinguan'), or a dwarf one (VD, M26). The 3D architecture-based RATP model was parameterized to estimate the canopy photosynthesis rate (*A_c*), transpiration rate (*E_c*), and *WUE_c*. Then, virtual scenarios were used to compare the relative contributions of cultivar and interstock to canopy *A_c*, *E_c*, and *WUE_c*. These scenarios changed the leaf distribution and functions of either cultivar or interstock. At the leaf scale, VD trees had significantly higher leaf nitrogen per area but a lower maximum carboxylation rate and dark respiration in both cultivars. In parallel with higher leaf stomatal conductance (*g_s*) and transpiration in VD 'Fuji' and similar *g_s* in VD 'Gala', VD trees showed significantly lower leaf photosynthesis rate and *WUE* than VV trees. However, lower leaf photosynthetic capacities in VD trees were compensated at the canopy scale, with *A_c* and *WUE_c* for 'Fuji' significantly improved in VD trees under both sunny and cloudy conditions, and for 'Gala' significantly improved in VD trees under cloudy conditions compared with VV trees. Switching scenarios highlighted that 'Gala' leaf functions and distribution and VD leaf distributions enhanced *A_c* and *WUE_c* simultaneously, irrespective of

weather conditions. Up-scaling leaf gas exchange to the canopy scale by utilizing 3D architecture-based modeling and reliable measurements of tree architecture and leaf functional traits provides insights to explore the influence of genetic materials and tree management practices.

KEYWORDS

Malus domestica, RATP model, stomatal conductance, leaf functional traits, dwarfing interstocks, virtual scenario, 3D architecture-based model

Introduction

Grafting is an ancient technique that assembles a composite plant in the form of a shoot system (the scion) grafted on a root system (the rootstock) (Fazio et al., 2015; Foster et al., 2016; Baron et al., 2019). Although the method was originally used for clonal propagation, it has been widely used in forestry and horticulture to induce dwarfing and attain resistance to disease and tolerance to abiotic stresses, such as drought, salinity, and extreme temperatures, to enhance water- and nutrient-use efficiency (Han et al., 2019; Migicovsky et al., 2019; Zhang et al., 2022a). As most dwarfing rootstocks are shallow-rooted and sensitive to stresses, grafting a dwarf interstem between the scion and stress-tolerant rootstock can take advantage of the strength of the rootstock and the dwarfing effect of the interstem, which is termed the ‘interstock’ (Di Vaio et al., 2009). This method enables the scion, interstock, and rootstock to be selected based on desired traits with the objective of maintaining the beneficial traits of all parts of the grafted plants. Thus, understanding scion–interstock/rootstock interactions will aid in improving scion or root architectural and physiological traits to increase productivity.

Fusion of the vascular systems occurs during the connection of the rootstock and scion and can be affected by both rootstock and scion genotypes (Baron et al., 2019). The root architecture is varied among rootstocks and can modify the graft vessel diameter or density in the graft union, both of which potentially affect scion water status (Tombesi et al., 2009; Albacete et al., 2015; Xu and Ediger, 2021). Several hypotheses for rootstock control of scion vigor have been proposed, involving nutrient uptake, hydraulic conductance, and hormone regulation (Webster, 1995; Solari et al., 2006; Tworokski and Miller, 2007; Van Hooijdonk et al., 2011). These changes lead directly to changes in leaf-scale gas exchange, through which photosynthesis provides the carbon essential for tree growth and reproduction. However, inconsistency in the influence of rootstocks on leaf gas exchange reported among previous studies (Barden and Ferree, 1979; Schechter et al., 1991; Jia, 1995; Fallahi et al., 2002; Sotiropoulos, 2008; Liu et al., 2012; An et al., 2017; Fullana-Pericàs et al., 2020; Zhou et al., 2020). In addition, tree growth and yield are associated with the sum of seasonal net canopy photosynthesis rather than the net leaf photosynthesis rate (A_l) of specific leaves of the canopy (Monteith, 1977). As a result, the photosynthesis and water use response to a rootstock or interstock must be upscaled from the leaf scale to the canopy scale.

At the canopy-scale, tree architecture is central to the tradeoff between canopy carbon gain and water use by influencing leaf area spatial distribution, intra-canopy microclimate (light, temperature, CO₂, and humidity), water transport, and carbon assimilation and allocation (Minas et al., 2018; Coupel-Ledru et al., 2022). Leaf stomatal control of photosynthesis and water loss by transpiration can interact with intra-canopy microclimate, particularly light, and result in acclimation of leaves by modifying photosynthesis related functional traits, such as dark respiration (R_d), nitrogen content per area (N_a), maximum rate of carboxylation (V_{cmax}), and maximum rate of electron transport (J_{max}) (Hikosaka, 2003; Bauerle et al., 2007; Poorter et al., 2019). In particular, the interstock/rootstock has a profound effect on tree architecture by regulating internode and shoot growth and canopy volume (Preston, 1967; Seleznyova et al., 2003; Costes and Garcia-Villanueva, 2007; Warschefsky et al., 2016), which directly affect the intra-canopy microclimate, heterogeneity of leaf-scale gas exchange, and related leaf functional traits within the canopy, and in turn alter energy exchange with the surrounding environment and resource use efficiencies of the canopy. Given the complexity of canopy structure, the current understanding of stomatal, photosynthesis, and water-use responses to scion–rootstock combinations is limited to pot experiments conducted in controlled environments to minimize the architecture effect, and such studies are rarely performed in field environments. Moreover, such variation in leaf functional traits and the coincident intra-canopy microclimate that are influenced by interstock/rootstock or scion genotypes are rarely taken into account.

Overall, a better understanding of scion–rootstock interactions must consider tree architecture and variability in intra-canopy microclimate and leaf functional traits induced by tree architecture, which demands a more efficient and accurate three-dimensional (3D) tree architecture-based modeling approach to represent complex relationships among the above-mentioned factors. Because of the intertwined effects between tree architecture and leaf functions, and that both are assumed to depend on interstock/rootstock and scion genotypes, it is crucial to decipher their respective effects on canopy-scale photosynthesis and water use.

Apple (*Malus × domestica*) is suitable for exploring scion–rootstock interactions owing to its high economic value, ease of cloning, diverse genetic resources, successful application of interstocks and rootstocks, and development of 3D architecture-

based models (Costes et al., 2008; Yang et al., 2021). Numerous 3D architecture-based plant models have been established to study complex relationships among tree architecture, canopy microclimate, transpiration, and carbon assimilation and allocation to screen the relative contribution of architectural and leaf functional traits to select ‘optimized’ combinations by conducting virtual experiments (Chen et al., 2014; Picheny et al., 2017; Zhu et al., 2019; Zhang et al., 2022b). However, rule-based plant architecture simulation is time-consuming and recreation of the large tree structure in the field is difficult (Zhu et al., 2019). Similarly, imaging and terrestrial light detection and ranging-based methods underestimate shoot number in apple trees and cannot detect shoots and leaves inside the canopy (Pallas et al., 2020). Alternatively, 3D tree reconstruction through combining partial 3D digitization of all leafy shoots within the canopy, allometric relationships, and random distribution of certain organ attributes is feasible to represent the large tree structure in the field (Massonnet et al., 2008; Yang et al., 2021). Thus, the radiation absorption, transpiration, and photosynthesis (RATP) model that uses 3D digitized trees as input has been successfully developed for large tree architectures to simulate the spatial distribution of radiation and leaf gas exchange within a canopy considering the canopy structure and microclimate as well as leaf physical and physiological properties (Sinoquet et al., 2001). This model has been applied to apple trees for exploring canopy water use, carbon assimilation (Massonnet et al., 2008; Yang et al., 2021), carbon allocation (Reyes et al., 2018), and within-canopy climate variability (Ngao et al., 2017; Woods et al., 2018).

In this study, we aimed to evaluate the relative impact of the variability of leaf functions and tree architecture on canopy performance in apple trees by comparing combinations of two cultivars and two interstocks. We measured leaf gas exchange and use the RATP model to determine whether there are differences among scion–rootstock combinations in photosynthetic capacities and water use at either leaf or canopy scales and in related physiological processes (V_{cmax} , J_{max} , and R_d) in response to the environment. Making use of this modeling approach, we performed virtual experiments to decipher the effects of leaf functions and leaf distribution as modulated by interstocks or cultivars on canopy performance. We tested all possible combinations of leaf properties (at the leaf scale) and distribution (at the canopy scale) to compare and evaluate canopy photosynthetic capacity and water use efficiency (*WUE*).

Materials and methods

Plant materials

The experiment was conducted at an extension station of the National Apple Industry Technology System of the Agriculture Ministry of China, Fengxiang, situated at 806 m above sea level with mean annual precipitation of 532.5 mm. In winter 1998, two apple cultivars, ‘Liquan Fuji’ (hereafter ‘Fuji’) and ‘Regal Gala’ (hereafter ‘Gala’), were grafted onto a vigorous, drought-tolerant *M. micromalus* rootstock, in combination with two interstocks: *M.* ×

domestica ‘Qinguan’, a vigorous interstock (hereafter ‘VV’), and M26, a dwarf interstock (hereafter ‘VD’). All trees were trained in accordance with the spindle training system with a 3.0–3.5 m tree height and all scaffold branches tied down below horizontal (100–120° from vertical). The length of the interstocks was 30 cm, and the grafted points were 10 cm above the soil for all trees. Trees were planted 2.0 m × 3.5 m apart in a north–south orientation. Horticultural practices included regular irrigation with mini-sprinklers, standard fertilization, and phytosanitary treatments. During the growing seasons of the experiment, all trees were left unpruned but were pruned in the winter. Fruit thinning was performed each year according to professional practices to adjust the crop load within 2.42 ± 0.20 fruits per trunk cross-sectional area (*TCSA*, cm²). The leaf area index (*LAI*) was calculated as the ratio of total leaf area (estimated from the virtual canopy) to tree spacing.

Tree measurement and 3D digitizing

The *TCSA* is a stable index of tree vigor (Strong and Azarenko, 2000) and was estimated from the trunk circumference measured with a tape for five trees during winter for each treatment and in 2011 and 2012. In addition, canopy structures were digitized after 190 DOY (day of year) when shoots growth were ceased. The spatial coordinates of the distal and proximal points of all current-year leafy shoots were collected using an electro-magnetic 3D digitizer (Polhemus; Colchester, VT, USA) and recorded with PiafDigit software (Donès et al., 2006). All shoots in the trees were classified based on their fate as apical meristems. The floral bud develops into a rosette (also termed a bourse) with non-elongated internodes at the base and an inflorescence in the terminal position (Pratt, 1988). The bourse may give rise to one or two bourse shoots that develop immediately (Lauri et al., 1995). In addition, vegetative shoots develop from vegetative buds. A threshold of 5 cm was used to discriminate long and short shoots (Costes et al., 2006). After tree digitization, at least 15 randomly selected shoots per shoot type for each treatment in each year were digitized at the leaf scale to determine leaf Euler angles (midrib azimuth and elevation, and lamina rolling around the midrib), and the angles between the leaf petiole and shoot axis according to Farque et al. (2001). All sampled shoots were transported to the laboratory to measure the shoot length with a ruler and count the leaf number. Moreover, a non-destructive leaf photo scanner was used to obtain images of all leaves from the sampled shoots. The leaf width, leaf length, and leaf area were digitally processed using ImageJ software (1.48q 1 February 2014, <https://imagej.nih.gov/ij/>). Each leaf was labeled with information about the year, cultivar, interstock, shoot number, and node rank. Shoot leaf area was obtained by summing the leaf areas of leaves from the same shoot. Finally, the allometric relationships between the shoot length (*SL*) and shoot leaf area (*SLA*, equation 1), between the *SL* and the shoot leaf number (*SLN*, equation 2), between the leaf length (*LL*) and leaf area (*LA*, equation 3), between *LL* and leaf width (*LW*, equation 4), and between *LL* and petiole length (*PL*, equation 5) were established.

$$SLA = a_{SLA}SL + b_{SLA} \quad (1)$$

$$SLN = a_{SLN}SL + b_{SLN} \quad (2)$$

$$LA = a_{LA}LL^2 \quad (3)$$

$$LW = a_{LW}LL + b_{LW} \quad (4)$$

$$PL = a_{PL}LL + b_{PL} \quad (5)$$

where a_i and b_i are coefficients, and i denotes the identifier (SLA , SLN , LW , LA or PL) for each equation.

Distributions of leaf rolling and elevation angles were obtained based on the leaf Euler angles.

Reconstruction of a 3D virtual canopy

The spatial position and length of leafy shoots were determined by the spatial coordinates of the distal and proximal points. During reconstruction, the following principles were assumed: (1) SLA and SLN were estimated from SL based on equations 1 and 2, respectively; (2) all leaves attached to the same shoot were evenly distributed with an average LA and which was estimated as the ratio of SLA to SLN ; (3) all leaves were reconstructed as plane hexagons without considering the midrib curvature and folding angle of the lamina because their effects on light interception properties are weak (Génard et al., 2000); (4) LL was estimated from LA (equation 3), and LW (equation 4) and PL (equation 5) were estimated from LL and were used to calibrate the hexagonal shape; (5) petiole, midrib, and shoot axes were assumed to be in the same plane defined by the shoot axis direction and the phyllotactic angle β , which was constant and equal to the average values obtained in the field; (6) petiole insertion points along a shoot were evenly segmented with an average internode length (equal to the ratio of SL/SLN), and the connection point between the petiole and leaf was computed in accordance with the shoot coordinates, β , and PL . The connection point between the petiole and leaf was used as the coordinates of the lamina origin and leaf elevation and the rolling angle was determined from the angle distribution for each shoot type, and leaf azimuth angles were distributed following a 2/5 phyllotaxy. In total, 19 trees were generated, additional details are described by Yang et al. (2016). All fitting parameters for allometric relationships, leaf elevation and rolling angle distribution, angle between the leaf petiole and shoot axis, and all virtual canopies have been deposited in the Zenodo repository (<http://doi.org/10.5281/zenodo.4049858>).

Measurements of leaf gas exchange

Gas exchange was measured at the leaf scale using a portable photosynthesis system (LI-6400, Li-Cor, Lincoln, NE, USA) from 08:30 to 12:30 during 217 DOY (day of year) to 225 DOY for ‘Gala’ in 2013 and during 223 DOY to 231 DOY for ‘Fuji’ in 2018. A

preliminary report on the data collection for ‘Fuji’ in 2013 has been presented (Yang et al., 2019). Photosynthesis responses to intercellular CO_2 concentration (C_i) were based on 6–8 fully expanded leaves by modifying the ambient CO_2 concentration (C_a) in the leaf chamber in the following order: 400, 300, 200, 100, 50, 400, 600, 800, 1000, 1200, 1500, and 1800 $\mu mol mol^{-1}$; the other parameters were fixed at 1500 $\mu mol m^{-2} s^{-1}$ photosynthetic photon flux density (PPFD) using an integrated red-blue light source with 10% blue light, leaf temperatures at 30°C, and the vapor pressure deficit (VPD) between the leaf and air maintained below 1.5 kPa. The R_d was measured before sunrise (approximately 4:40–6:00). After the leaf was acclimated for 5–20 min per step to a steady state (changes in leaf stomatal conductance (g_{si}) less than $\pm 2\%$ over 2 min), gas exchange was recorded. The V_{cmax} and J_{max} were estimated from the leaf net photosynthesis rate (A_i)– C_i curve by fitting the biochemical model developed by Farquhar et al. (1980) and then were converted to values at 25°C based on parameters from Harley et al. (1992), which were obtained from barley chloroplasts (Nolan and Smillie, 1976). The spatial heterogeneity of V_{cmax} , J_{max} , and R_d within the canopy was predicted by linear functions depending on N_a , which was predicted by a linear function of the daily cumulated PPFD ($PPFD_d$). The $PPFD_d$ was measured with light sensors S-LIA-M003 (Onset Computers, Bourne, MA, USA) on leaves located along a gradient of irradiance within the canopy. The $PPFD_d$ in ‘Fuji’ was only measured in 2013.

Stomatal responses to PPFD, leaf temperature, and leaf surface VPD in the Jarvis model (Jarvis, 1976) were measured for a range of PPFDs (0–1500 $\mu mol m^{-2} s^{-1}$), temperatures (20–35°C), and VPDs (1.0–3.5 kPa). During measurements, only one environmental factor was altered and the other parameters were fixed at 1500 $\mu mol m^{-2} s^{-1}$ PPFD, leaf temperature at 30°C, and the VPD between the leaf and air was maintained below 1.5 kPa. Maximal stomatal conductance (g_{smax}) was calculated based on the g_s values above the 90% percentile under optimal environmental conditions ($800 \leq PPFD \leq 1500 \mu mol m^{-2} s^{-1}$, $20 \leq T \leq 30^\circ C$, $1.4 \leq VPD \leq 2$ kPa, and $C_a = 380 \mu mol mol^{-1}$) for all leaves. Leaf water use was represented by the leaf instantaneous WUE (WUE_i) and was computed as the ratio of A_i to leaf transpiration rate (E_i). Subsequently, the leaf area was measured on each leaf, and each leaf was oven-dried at 80°C to a constant weight and ground with a mortar. A subsample of 5.0 mg power was used to measure leaf nitrogen concentration using an automatic analyzer (FlowSys, Systea, Italy).

Meteorological variables

Meteorological variables measured comprised incident PPFD, air temperature (T), air relative humidity (RH), and wind speed at 2 m above the ground in the orchard. Total PPFD was measured with a S-LIA-M003 sensor, air T and RH with a S-THB-M008 sensor, and wind speed with a S-WSB-M003 sensor (Onset Computers, Bourne, MA, USA). All data were averaged and stored at time steps of 1 min in a HOBO U30 data logger (Onset

Computers). Inputs of incident radiation into RATP included atmospheric radiation, direct and diffuse PPFD, and near-infrared radiation (NIR). As only total PPFD was measured, atmosphere radiation was estimated in accordance with Brutsaert (1975), and diffuse/direct PPFD were estimated in accordance with Spitters et al. (1986) and Marco Bindi et al. (1992) based on measured climate data in an orchard. The NIR was assumed to have the same diffuse/direct ratio as PPFD. The number of directions of diffuse light interception computation was 46 and air CO₂ concentration was 380 ppm during the simulation.

Estimation of photosynthesis and transpiration at canopy scale

The canopy net daily photosynthesis rate per leaf area per day (A_c , mmol m⁻² d⁻¹, equation 6) and transpiration rate per leaf area per day (E_c , mol m⁻² d⁻¹, equation 7) were calculated by integrating the diurnal instantaneous canopy photosynthesis rate (A_h , μmol m⁻² s⁻¹) and transpiration rate (E_h , mmol m⁻² s⁻¹) which were simulated from isolated trees using the RATP model (available at <http://www.openalea.gforge.inria.fr>) (Pradal et al., 2008).

$$A_c = \sum_{h=0.5}^{h=24} A_h \cdot 30 \cdot 60 \cdot 10^{-3} \quad (6)$$

$$E_c = \sum_{h=0.5}^{h=24} E_h \cdot 30 \cdot 60 \cdot 10^{-3} \quad (7)$$

where 30 is the simulation step in 30 min and 10⁻³ is the unit conversion from μmol to mmol for A_c and from mmol to mol for E_c . Canopy WUE (WUE_c) was computed as the ratio of A_c to E_c . The simulation was run from 190 DOY to 273 DOY, when all shoot growth had ceased, and then those days with PPFD_d more than 45 mol m⁻² d⁻¹ and less than 15 mol m⁻² d⁻¹ were classified as sunny and cloudy days, respectively. Key parameters used for the RATP model are listed in Supplementary Table 1.

Analysis of virtual scenarios

The setting of virtual experiments was conducted as proposed by Massonnet et al. (2008) (Table 1). The simulation with the actual leaf distribution and functions for each treatment was the reference S0 scenario. The S1 scenario is that in which leaf functional parameters were switched between 'Fuji' and 'Gala' with the same interstock/rootstock combination. In the S2 scenario, leaf functional parameters for the same cultivar were switched between VV and VD. Starting with VD trees (S0a-b and S1e-f), the effect of foliage distribution on the two cultivars was evaluated by comparing S0a and S1e with S0b and S1f for 'Gala' and 'Fuji', respectively. To evaluate the effect of leaf functions on the two cultivars, S0a and S1f were compared with S0b and S1e for 'Gala' and 'Fuji' effects. Comparing S0c and S1g with S0d and S1h, and S0c and S1h to S0d and S1g, respectively, allowed us to perform similar analyses on VV trees. In the S2 scenario, the effects of interstocks were deciphered in a similar manner.

Statistical analyses and model validation

All data were analyzed using the R software (R Development Core Team, 2020). The linear and non-linear relationships between measurements and/or parameters were fitted with 'lm' and 'nls' functions, respectively. We performed linear modeling using the *lm* () function in R, accounting for variation in interstock, cultivar, and their interaction. The percent variance explained by each factor was calculated using the *anova*() function, and only those with a significant *P* value (<0.05) were visualized using the *ggplot2* package. After ANOVAs, significant differences among treatments were distinguished by the Duncan multiple mean comparison test at the *P*< 0.05 level using the *agricolae* package. To test if there were differences between interstocks, the ANCOVA for differences in the slope and intercept of linear relationships was performed.

TABLE 1 Reference (S0) and switching scenarios (S1 and S2) obtained with the RATP model for 'Fuji' and 'Gala' apple trees grafted on vigorous rootstocks and associated with either a dwarf M26 interstock (VD) or a vigorous 'Qinguan' interstock (VV).

| Scenario | Leaf distribution | Leaf function | Order of leaf distribution × function combination |
|----------|-------------------|---------------|---|
| S0 | VD Fuji | VD Fuji | a |
| | VD Gala | VD Gala | b |
| | VV Fuji | VV Fuji | c |
| | VV Gala | VV Gala | d |
| S1 | VD Fuji | VD Gala | e |
| | VD Gala | VD Fuji | f |
| | VV Fuji | VV Gala | g |
| | VV Gala | VV Fuji | h |
| S2 | VD Fuji | VV Fuji | i |
| | VD Gala | VV Gala | j |
| | VV Fuji | VD Fuji | k |
| | VV Gala | VD Gala | l |

The quality of the Farquhar and Jarvis sub-models' parameterization was assessed by calculating the root mean square error (RMSE, equation 8) and relative root mean square error (RRMSE, equation 9), indicators of the overall relative accuracy of a model.

$$RMSE = \sqrt{\frac{\sum_{i=1}^n (O_i - S_i)^2}{n}} \quad (8)$$

$$RRMSE = \frac{RMSE}{\bar{O}} \times 100 \quad (9)$$

where O_i is the observed value and S_i is the simulated value. The smaller the RMSE and RRMSE, the more accurate the simulation. In this study, model accuracy is considered excellent when $RRMSE < 10\%$; good if $10\% \leq RRMSE < 20\%$; fair if $20\% \leq RRMSE < 30\%$; and poor if $RRMSE \geq 30\%$ (Li et al., 2013).

Results

Leaf-scale photosynthesis, transpiration, and WUE

Although there was strong variability in A_i , E_i , and WUE_i , the mean values were significantly affected by cultivar, interstock, and their interactions (Figure 1). Leaf A_i variation was significantly explained (20.7%) solely by interstock, with A_i higher in VV than in VD (+14.5% and +19.7% for 'Fuji' and 'Gala', respectively) (Figures 1A, D). The variation in E_i and WUE_i was significantly explained by both cultivar (18.5% for E_i and 18.7% for WUE_i) and interstock (32.3% for E_i and 50.1% for WUE_i), and their interaction significantly explained 5.67% of the variation for E_i (Figure 1D). The VD trees had higher E_i in both 'Fuji' and 'Gala' (+60.4% and +24.4%) and lower WUE_i in both 'Fuji' and 'Gala' (−45.6% and −31.4%) than VV trees (Figures 1B, C).

Leaf stomatal conductance and responses to environmental factors

As responses of leaf g_s/g_{smax} at leaf scale to environmental conditions and depending on interstocks were mostly consistent between cultivars for the Farquhar's and Jarvis' model parameters, results for 'Gala' are presented afterward, except when significant differences were found between cultivars.

The slopes of the linear relationship between g_{smax} and N_a in 'Gala' and 'Fuji' were significantly affected by interstock variation, with VD trees having larger slopes than VV trees in both cultivars (Figure 2; Supplementary Figure 1). The effect of interstock on the intercept of the linear relationship between g_{smax} and N_a in 'Gala' was not significant, but it was significant for 'Fuji'.

The g_s/g_{smax} responses to environmental factors are shown in Figure 3 and Supplementary Figure 2. The g_s/g_{smax} values continuously increased from 0 to the highest PPFd, irrespective of interstock. The optimal temperature was approximately 27°C for both VD- and VV-Gala, but higher values of 29.1°C for VD-Fuji and 31.8°C for VV-Fuji were found. The g_s/g_{smax} remained high under increasing VPD until a threshold was attained. The VPD threshold was significantly higher in VV-Gala than in VD-Gala (1.46 and 1.86 kPa for VD-Gala and VV-Gala, respectively; $P < 0.05$). Beyond the threshold, g_s/g_{smax} was significantly negatively correlated with VPD, irrespective of scion–interstock combinations. An ANCOVA test showed that there were significant differences in the regression intercepts between g_s/g_{smax} with VPD for VV vs. VD, irrespective of cultivar, with higher g_s/g_{smax} in VD than VV at the same point on the x-axis.

Leaf nitrogen and V_{cmax} , J_{max} , and R_d

Along the light gradient within the canopy, the leaf N_a decreased and was significantly positively correlated with the PPFd, irrespective of cultivar and interstock (Figure 4;

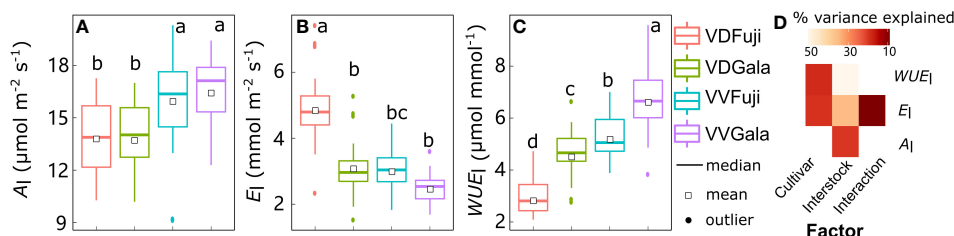


FIGURE 1

Boxplot of the leaf scale net photosynthesis rate (A_i) (A), transpiration (E_i) (B), and water use efficiency (WUE_i) (C) in 'Fuji' and 'Gala' apple trees grafted on vigorous rootstocks associated either with a dwarf M26 interstock (VD) or a vigorous 'Qinguan' interstock (VV), and the corresponding amount of variance explained by cultivar, interstock, and their interactions (D). The percent variance explained by each factor in the model is indicated using color for those factors which explain a significant portion of the variance ($p < 0.05$).

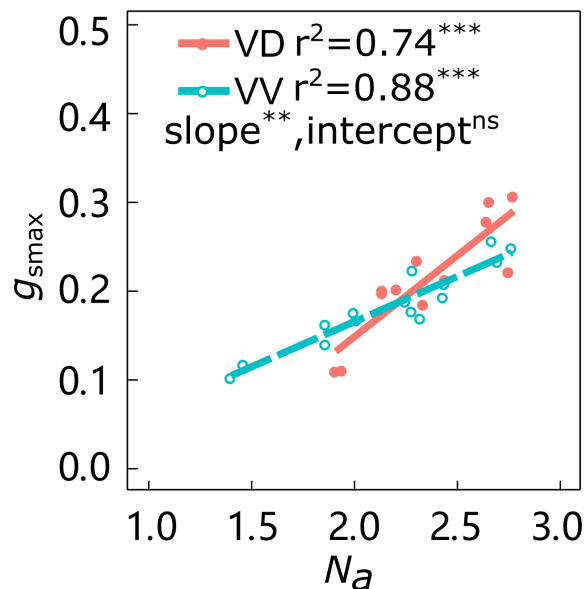


FIGURE 2
Relationships between leaf nitrogen content per area (N_a) and maximum stomatal conductance (g_{smax}) of ‘Gala’ apple trees grafted on vigorous rootstocks and associated with either a dwarf M26 interstock (VD) or a vigorous ‘Qinguan’ interstock (VV). Linear regression coefficients (r^2) and significance for the regression slope and intercept are shown when $P < 0.01$ with ** and $P < 0.001$ with *** and ns means no significant difference between interstocks.

Supplementary Figure 3). An ANCOVA test showed that there were significant differences in intercepts between $PPFD_d$ and N_a in both ‘Fuji’ and ‘Gala’, and in slopes for ‘Fuji’ for VV vs. VD trees. The VD trees had a greater N_a than VV for a given $PPFD_d$, irrespective of cultivar, indicating that the VV had a greater reduction of N_a than VD through decreasing light.

As expected, leaf N_a was significantly positively correlated with V_{cmax} and J_{max} in all treatments, and negatively correlated with R_d (Figure 5; Supplementary Figure 4). The regression intercepts between V_{cmax} , J_{max} , and R_d with N_a were significantly different for VV vs. VD in both ‘Fuji’ and ‘Gala’, indicating greater V_{cmax} , J_{max} and R_d (in absolute values) in VV than in VD trees for a given N_a in both cultivars (except J_{max} for ‘Fuji’; Supplementary Figure 4B). In

addition, a significantly different slope was observed only between V_{cmax} with N_a for VV vs. VD in ‘Gala’; the remainder of the corresponding regression slopes were not significantly different for VV vs. VD in both ‘Fuji’ and ‘Gala’, indicating higher sensitivity of V_{cmax} to N_a for VD than VV in ‘Gala’. Leaf mass per area (LMA) is a central trait within the leaf economics spectrum and is tightly coupled with leaf photosynthetic traits. The LMA was significantly positively correlated with $PPFD_d$, irrespective of cultivar and interstock (Supplementary Figure 5). An ANCOVA test showed that there was a significant difference in slope between $PPFD_d$ with LMA in ‘Fuji’ only for VV vs. VD trees. Interstock had no effect on the intercept of the linear relationship between $PPFD_d$ with LMA in both ‘Fuji’ and ‘Gala’ for VV vs. VD trees.

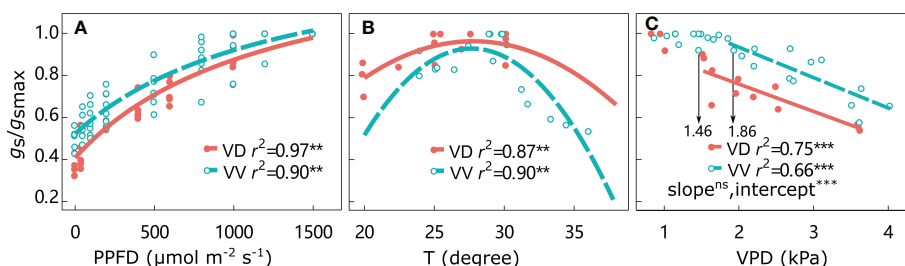


FIGURE 3
Relative stomatal conductance g_s/g_{smax} responses to photosynthetically active radiation (PPFD) (A), temperature (T) (B), and water vapor pressure deficit (VPD) (C) for ‘Gala’ apple trees grafted on vigorous rootstocks and associated with either a dwarf M26 interstock (VD) or a vigorous ‘Qinguan’ interstock (VV) for the whole tree. The threshold VPD values ensuring $g_s = g_{smax}$ are presented. Regression coefficients (r^2) for all fitted lines, linear regression significance and interstock effect on a slope and intercept for VPD are shown when $P < 0.01$ with ** and $P < 0.001$ with ***.

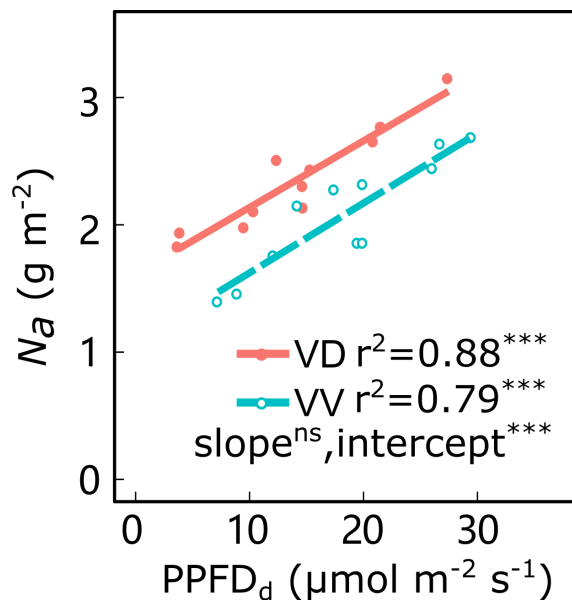


FIGURE 4

Relationships between daily cumulated photosynthetic photon flux density ($PPFD_d$) and leaf nitrogen content per area (N_a) for 'Gala' apple trees grafted on vigorous rootstocks associated either with a dwarf M26 interstock (VD) or a vigorous 'Qinguan' interstock (VV). Linear regression coefficients (r^2) and significance and interstock effect on slope and intercept are shown when $P < 0.001$ with *** and no significant difference with ns.

Canopy architecture, photosynthetic capacities, and *WUE*

Leaf spatial distributions based on the 3D canopy were represented for 'Fuji' and 'Gala' in the two interstock/rootstock combinations (Figure 6). The LAI in VD trees was significantly lower (-33.2%) than in VV trees for 'Fuji' ($P < 0.05$), but were not significantly different between VD and VV trees for 'Gala'. In addition, the tree vigor (represented by $TCSA$) in VD trees was significantly higher than that in VV trees (-37.1% and -47.0% for 'Fuji' and 'Gala', respectively), irrespective of the cultivar (Supplementary Figure 6).

For the reference scenario (S0), the g_{sl} and A_l values predicted by the RATP model and the measured values were in good

agreement with low RMSE ($0.0476 \text{ mol m}^{-2} \text{ s}^{-1}$ and $1.90 \text{ μmol m}^{-2} \text{ s}^{-1}$ for g_{sl} and A_l , respectively) and RRMSE (19.6% and 14.1% for g_{sl} and A_l , respectively) values (Figure 7). Based on the of RRMSE values, the model showed good performance in predicting g_{sl} and A_l .

Following the accurate predictions of leaf-scale gas exchange, the A_c , E_c , and WUE_c under both sunny and cloudy conditions were simulated with the RATP model (Figure 8). According to the estimations provided by the RATP model, variation in A_c , E_c , and WUE_c was significantly explained by cultivar, interstock, and their interactions (Figure 8G, except for the interstock effect on A_c under sunny conditions and WUE_c under cloudy conditions). Although the cultivar explained similar variation in A_c between sunny (43.6%) and cloudy (45.5%) conditions, variation in E_c and WUE_c explained

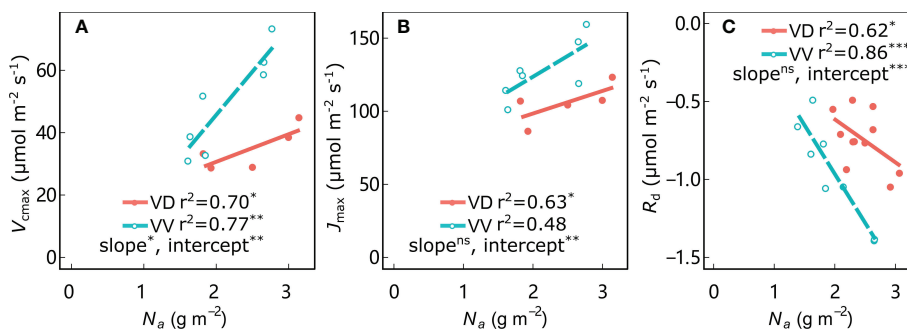


FIGURE 5

Relationships between maximum rates of carboxylation (V_{cmax}) (A), maximum rates of electron transport (J_{max}) (B), and dark respiration (R_d) (C) with leaf nitrogen content per area (N_a) for 'Gala' apple trees grafted on vigorous rootstocks associated with either a dwarf M26 interstock (VD) or a vigorous 'Qinguan' interstock (VV). Linear regression coefficients (r^2) and significance and interstock effects on slopes and intercepts are shown by the level of significance of the p-values: *significant at $0.01 \leq P < 0.05$; **significant at $0.001 \leq P < 0.01$; ***significant at $P < 0.001$ and no significant difference with ns.

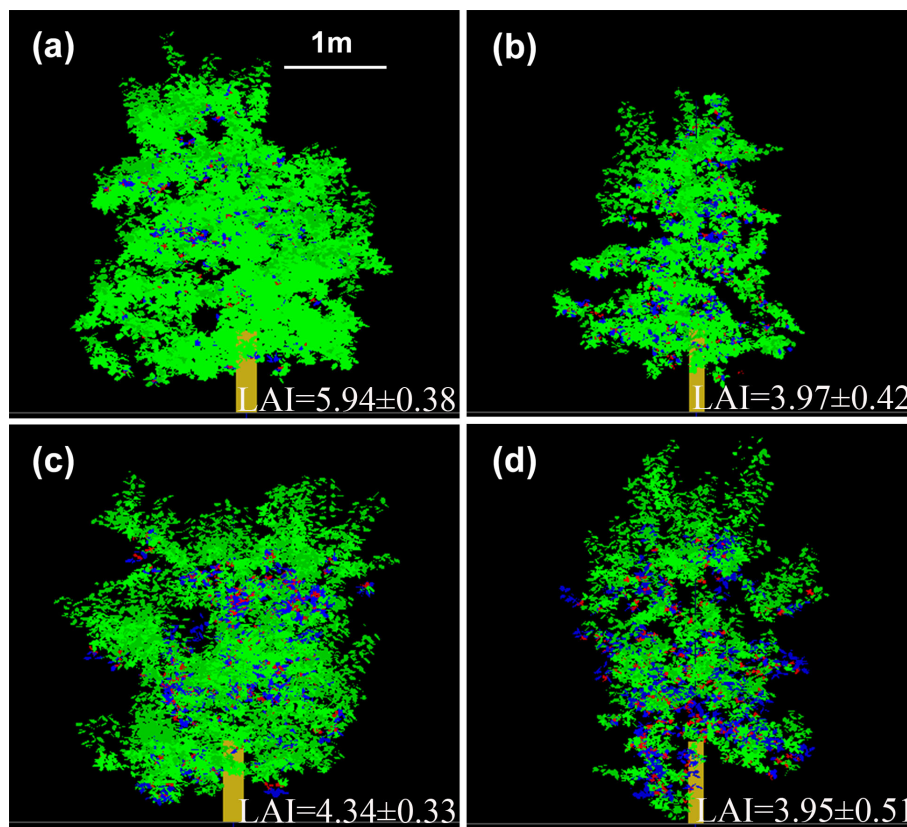


FIGURE 6
 Three-dimensional representation of 'Fuji' (A, B) and 'Gala' (C, D) trees grafted on vigorous rootstocks associated with either a dwarf M26 interstock (VD, (B, D) or a vigorous 'Qinguan' interstock (VV, (A, C). Leaf area index is given for each treatment. Virtual images were visualized with VegeSTAR software.

by the cultivar decreased from 34.5% under sunny to 8.32% under cloudy conditions for E_c and from 63.1% under sunny to 24.7% under cloudy conditions for WUE_c . In addition, interstock had a more significant influence on A_c under cloudy (18.9%) than sunny (0.058%) conditions.

Between cultivars grafted onto the same interstock, 'Gala' had significantly higher A_c and WUE_c than 'Fuji', irrespective of weather conditions (Figures 8A, C, D, F). Under sunny conditions, the A_c for 'Fuji' in VD trees was significantly greater (+24.7%) than that in VV trees, and this increased to +92.6% under cloudy conditions.

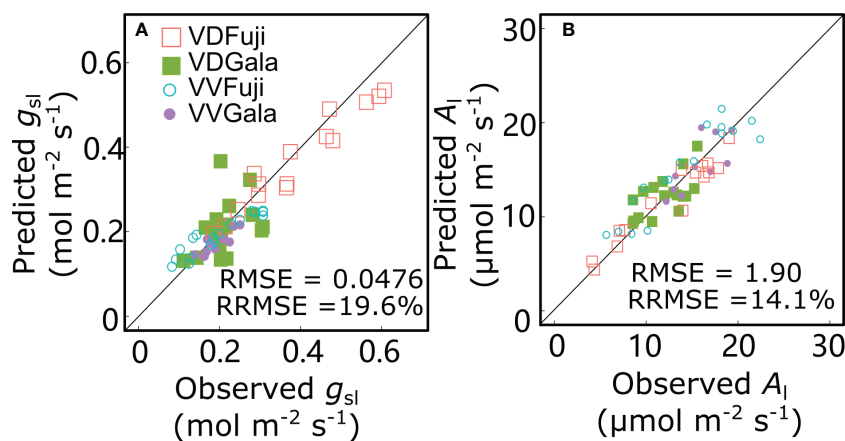
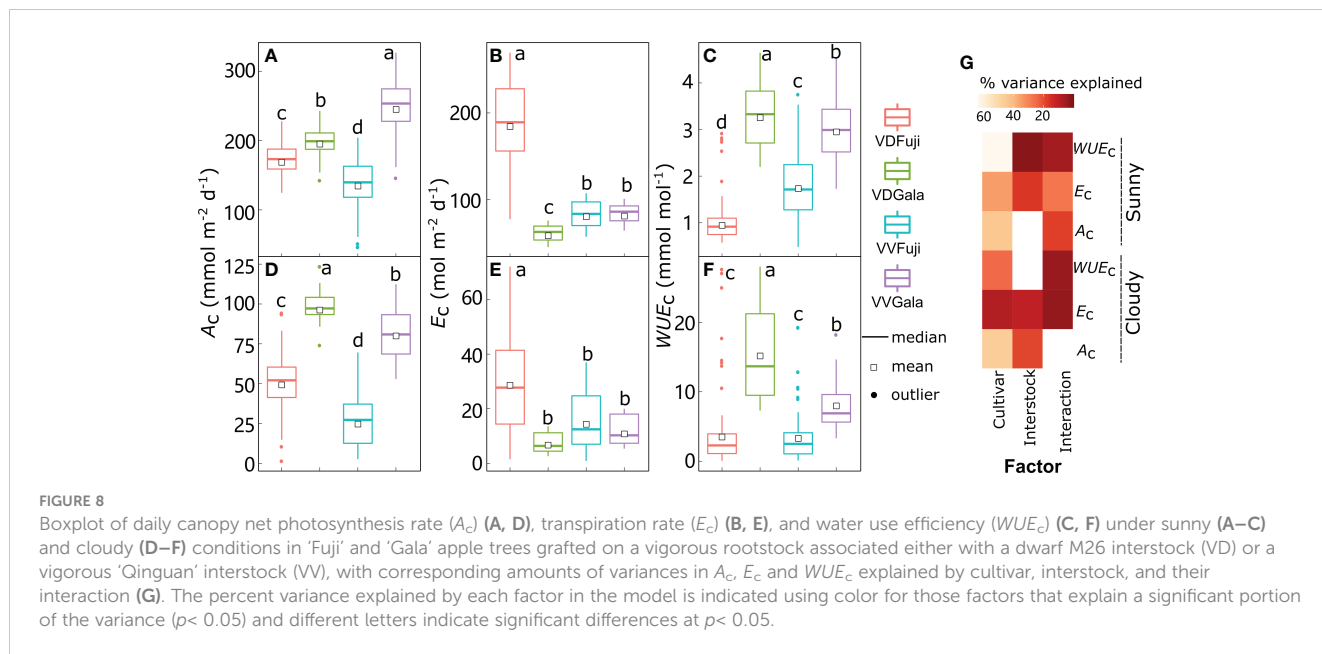


FIGURE 7
 Relationships between observed and predicted stomatal conductance (g_{sl}) (A) and net photosynthesis rate (A_l) (B) for 'Fuji' and 'Gala' apple trees grafted on vigorous rootstocks associated with either a dwarf M26 interstock (VD) or a vigorous 'Qinguan' interstock (VV). Each point represents one measurement/simulation at the leaf level. The 1:1 lines are represented.

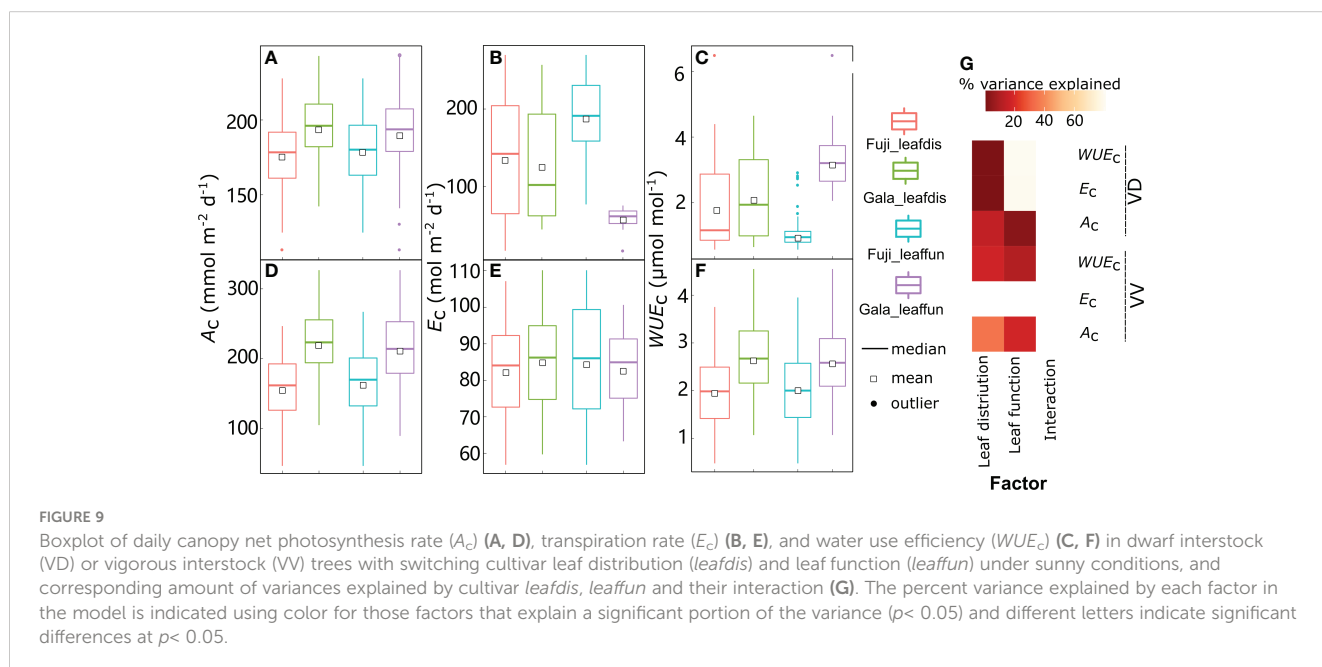


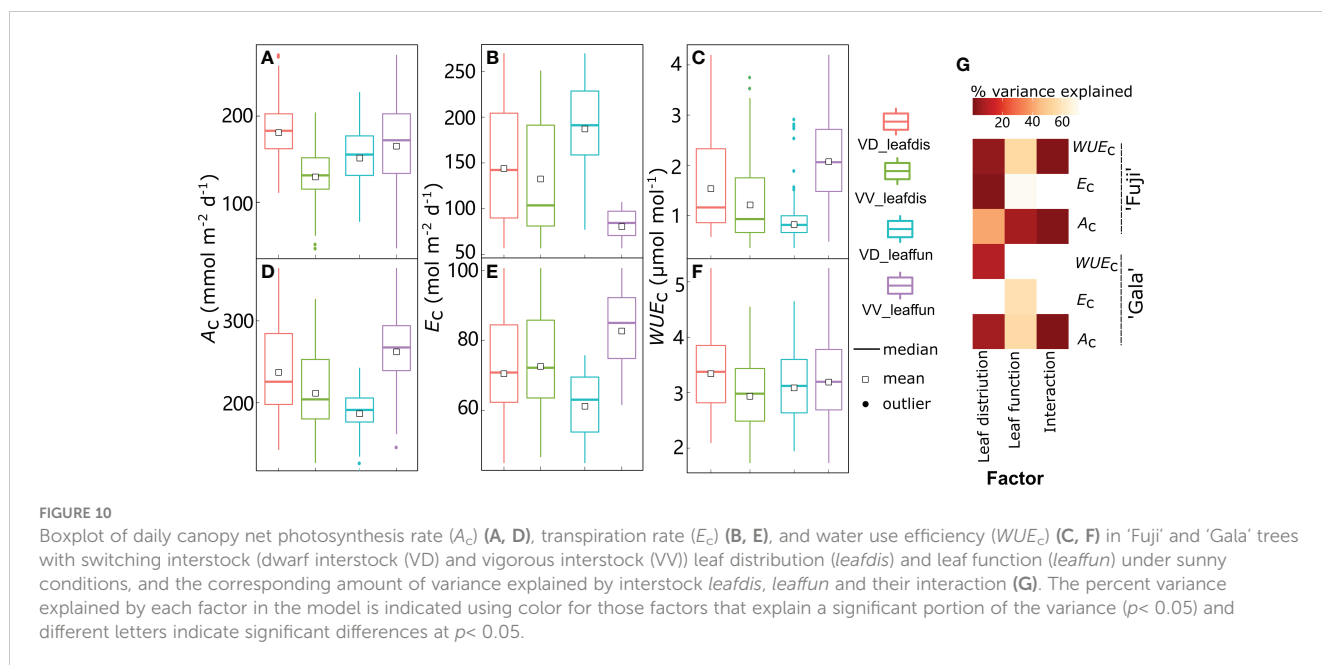
Furthermore, the E_c for ‘Fuji’ was significantly higher (+125%) in VD trees than in VV trees, which decreased to +92.8% in cloudy conditions (Figures 8B, E). Thus, the WUE_c for ‘Fuji’ in VD was significantly lower (–44.0%) than that of VV trees in sunny conditions and decreased in cloudy conditions with VD, whereas VV trees had similar WUE_c (Figures 8C, F). For ‘Gala’, the A_c in VD trees was –19.5% and –27.3% less than VV under sunny conditions, and inversely, +19.9% larger than VV trees under cloudy conditions (Figures 8A, D). In addition, the E_c in VD–Gala was –27.3% less than that in VV–Gala under sunny conditions, and even smaller with VV trees under cloudy conditions (Figures 8B, E). Unsurprisingly, the VD–Gala had a significantly larger WUE_c than the VV–Gala (+11.3% under sunny conditions and +85.8%

under cloudy conditions), irrespective of weather conditions (Figures 8C, F).

Relative contributions of leaf function and leaf distribution on canopy photosynthetic capacities and WUE

Scenario analyses showed that A_c , E_c , and WUE_c were modified by switching leaf distribution or functions compared with the reference S0 (Figure 8), but the amplitude of effects depended on the cultivar (Figure 9 under sunny conditions and Supplementary Figure 7 under cloudy conditions) or interstock (Figure 10 under





sunny conditions and [Supplementary Figure 8](#) under cloudy conditions).

By comparing scenarios S0 and S1, the relative roles of leaf distribution and functions were disentangled between 'Gala' and 'Fuji' in VV and VD trees under sunny conditions, respectively ([Figure 9](#)). Under sunny conditions, variation in A_c and WUE_c for both VV and VD trees and E_c for VD trees were significantly explained by both foliage distribution and function depending on the cultivar but without any interaction effects between cultivar leaf distribution and function, regardless of the variable considered to be significant ([Figure 9G](#)). Although variation in E_c was significantly explained by both leaf function (78.8%) and leaf distribution (0.37%) depending on the cultivar in VD trees, the latter contributed much less than the former. The A_c was significantly higher with 'Gala' leaf distribution (10.3% in VD and +40.6% in VV) or function (6.19% in VD and +29.4% in VV) compared with 'Fuji' ([Figures 9A, D](#)). In contrast, E_c was lower when considering 'Gala' rather than 'Fuji' leaf distribution (-6.51%) or functions (-68.2%), but this decrease was significant in VD trees only ([Figures 9B, E](#)). These resulted in notably higher WUE_c when considering 'Gala' leaf distribution (16.9% in VD and +34.0% in VV) or function (221% in VD and +27.2% in VV) than 'Fuji' ([Figures 9C, F](#)). Under cloudy conditions, both A_c (0.935–133 $\text{mmol m}^{-2} \text{d}^{-1}$) and E_c (0.661–80.0 $\text{mol m}^{-2} \text{d}^{-1}$) ranges showed significant decreases, whereas WUE_c (0.0117–36.4 mmol mol^{-1}) ranges showed significant increases compared with sunny conditions (46.3–364 $\text{mmol m}^{-2} \text{d}^{-1}$, 17.5–270 $\text{mol m}^{-2} \text{d}^{-1}$ and 0.350–6.49 mmol mol^{-1} for A_c , E_c and WUE_c , respectively) ([Figure 9](#), [Supplementary Figure 7](#)). Switching cultivar leaf distribution and function had consistent results under cloudy days, with the exception of the leaf distribution effect on E_c in VD trees, which was not significant but was significant under sunny

days ([Supplementary Figure 7](#)). The percentage increases with 'Gala' vs. 'Fuji' leaf distribution in A_c on cloudy days were 3.54- and 2.37-fold greater than on sunny days, respectively, and the percentage increases with 'Gala' vs. 'Fuji' leaf function in A_c on cloudy days were 11.0- and 2.26-fold greater than on sunny days.

By comparing scenarios S0 and S2, the relative roles of leaf distribution and functions generated by VV and VD interstocks were disentangled in 'Gala' and 'Fuji' under sunny conditions, respectively ([Figure 10](#)). Under sunny conditions, interstock leaf distribution influenced A_c and WUE_c ; VD trees showed significantly higher values in both cultivars, although the difference was more pronounced in 'Fuji' (+38.8% and 25.6% for A_c and WUE_c , respectively) than 'Gala' (+11.9% and 13.7% for A_c and WUE_c , respectively) ([Figures 10A, C, D, F](#)). Moreover, the leaf distribution owing to interstock explained a minor but significant 0.83% of the variance for E_c in 'Fuji' only, with VD trees showing 8.41% higher E_c than VV trees ([Figures 10B, E, G](#)). Regarding leaf functions, 'Fuji' trees with VV leaf functions had significantly higher A_c (+8.96%) and lower E_c (-56.0%), leading to significantly higher WUE_c (+143%) compared with VD leaf functions ([Figures 10A, B, C, G](#)). For 'Gala', trees with VV leaf functions had significantly higher A_c (39.0%) at the expense of higher E_c by a similar percentage (+34.8%) than trees with VD leaf functions, resulting in consistent WUE_c between VD and VV functions ([Figures 10D, E, F, G](#)). The interaction between leaf distribution and functions linked to interstock was significant for A_c and WUE_c in 'Fuji' and for A_c in 'Gala'. Consistent with the results under sunny days, the distribution of VD leaves was more conducive to the improvement of A_c and WUE_c than VV leaf distribution ([Supplementary Figure 8](#)). More importantly, the percentage increase with VD over VV leaf distribution in A_c and WUE_c under cloudy days was 2.15- and 1.58-fold for 'Fuji', and 1.36- and 3.59-fold for those under sunny days.

Discussion

Interstocks affect leaf photosynthetic parameters through nitrogen distribution and partition

In the current study, we considered adult apple trees in fruiting years and discovered that the VD trees had lower leaf photosynthetic capacity than the VV trees, regardless of the cultivar. In parallel, significantly higher leaf N_a was observed in VD trees than in VV trees, consistent with previous results obtained under similar conditions (Aguirre et al., 2001; Fallahi et al., 2002; Samuolienė et al., 2016) and in other fruited trees, such as cherry (Gonçalves et al., 2006) and grapevine (Sharma et al., 2016).

Nitrogen is the primary component of nucleotides and proteins essential for plant photosynthesis, key enzymes, and acclimation to light across numerous species (Evans, 1989; Niinemets et al., 2015). In the present study, the relationships observed between N_a and PPFD_d and between N_a and photosynthetic parameters (V_{cmax} , J_{max} and R_d) (Figures 4, 5) were consistent with previous studies (Le Roux et al., 2001; Walcroft et al., 2002; Massonnet et al., 2007; Niinemets et al., 2015) and in agreement with the optimization theory (Hirose and Werger, 1987). These relationships appeared robust and stable, regardless of the interstock. The range of V_{cmax} and J_{max} (Figures 5, 6) was also consistent with results reported for apple trees in other regions (Cheng and Fuchigami, 2000; Greer, 2014), but the values were smaller than those reported by Massonnet et al. (2007), likely because of climatic differences or changes in tree development during the growing season (Walker et al., 2014).

To interpret the lower leaf photosynthetic capacity together with the higher leaf N_a content in VD trees than in VV trees, three assumptions can be proposed. First, the reduction of both V_{cmax} and J_{max} in VD trees (except for J_{max} in VD–Fuji trees) suggests that nitrogen partitioning into carboxylation (mainly by Rubisco) and bioenergetics (associated with electron transport) could be lower in VD than in VV trees. A second hypothesis could be that leaf nitrogen is in excess, which might reduce Rubisco activity, whereas nitrogen could serve as a storage protein (Cheng and Fuchigami, 2000). A third hypothesis is that trees grafted on a dwarf rootstock have impaired sensing of the balance between starch reserves and cellulose and hexose sugars, resulting in higher starch concentrations in the leaves. This has been demonstrated in ‘Royal Gala’ when grafted on dwarf M9 rootstock compared with a vigorous ‘Royal Gala’ rootstock (Foster et al., 2017). Consequently, leaves in trees with a dwarf interstock are expected to have higher starch content that, in turn, could inhibit their photosynthetic capacity (Wünsche et al., 2005). However, disentangling these three assumptions or their possible combinations requires further investigation.

Moreover, R_d was smaller in VD trees than in VV trees, with values reported to be positively correlated with photosynthetic capacity, N_a , and LMA, and proportional to V_{cmax} (Farquhar et al., 1980; Niinemets and Tenhunen, 1997). In the current case, the decrease of R_d in VD trees was associated with LMA in ‘Fuji’ but

not in ‘Gala’, where LMA was not affected by interstock, nor with an increase of N_a as discussed above. We thus considered that the lower dark respiration was linked to the decrease in leaf biochemical potential (V_{cmax}) in both cultivars and associated with LMA in ‘Fuji’. This reflects the different response of a cultivar to the same interstock/rootstock.

Trees with vigorous interstocks appear less sensitive to abiotic stresses than dwarf interstock trees owing to slower stomata closure

The stomata adjust their aperture in response to environmental factors, leading to different tree *WUE*s. In the present study, we showed that dwarfing interstock induced faster stomatal closure when environmental conditions became stressful (i.e., high temperature, high VPD, and low light). In parallel, g_s/g_{smax} remained higher in VV trees than in VD trees. The relationships between g_s/g_{smax} and environmental factors were consistent with previous reports for apple (Dragoni et al., 2004; Massonnet et al., 2007) and walnut (Le Roux et al., 1999). This suggests that scions grafted on a vigorous interstock trees are able to maintain photosynthesis.

The g_{sl} and E_1 in VD–Fuji were higher than in VV–Fuji (Figure 1 and Supplementary Figure 1). However, dwarfing rootstocks may induce higher (Clearwater et al., 2004; Xu and Ediger, 2021) or lower g_{sl} and E_1 (Higgs and Jones, 1990; Cohen and Naor, 2002) than vigorous rootstocks. Hydraulic resistance in different parts of the soil–root–graft union–stem–leaf continuum has been proposed to regulate water transport, leaf gas exchange, and dwarfing (Olien and Lakso, 1986; Higgs and Jones, 1990; Cohen and Naor, 2002; Cohen et al., 2007; Tworkoski and Fazio, 2015). In the current study, the scion was grafted on an interstock/rootstock combination. Thus, the differences in g_{sl} and E_1 in ‘Fuji’ between interstocks may reflect differences in hydraulic architecture induced in the scion stem by the interstock/rootstock. However, given that such a difference was not observed in ‘Gala’, in which g_{sl} and E_1 were similar between interstocks, this might be due to differences in the response between scion–interstock/rootstock (Baron et al., 2019) and measurement periods between the two cultivars. Indeed, leaf gas exchange was measured near harvest for ‘Gala’, when g_{sl} decreases significantly (Greer, 2019), whereas it was performed before harvest for ‘Fuji’. A modeling approach that integrates the responses of g_{sl} and E_1 to root characteristics, hydraulic conductance, and chemical signals (Peccoux et al., 2018) would help to investigate the mechanisms of rootstock control on transpiration in apple trees.

At the leaf scale, WUE_1 depends on both A_1 and water loss through stomata. Indeed, higher stomatal conductance and photosynthesis are often followed by greater water use and carbon gain (Condon et al., 2004). Reduced A_1 in both cultivars resulted in lower WUE_1 in VD- rather than VV- trees. In ‘Fuji’ trees, this reduction was enhanced by higher E_1 in trees with VD interstock. This suggests that the tradeoff between A_1 and g_{sl} was

altered by interstock but depends on the cultivar. In this case, the higher g_{sl} may be responsible for the higher yield potential in dwarfing apple trees, as observed in crop species (Blum, 2005).

Upscaling from leaf to canopy scale, VD-Gala had lower E_c than VV-Gala but their LAI (Figure 6) and light interception efficiency (Yang et al., 2016) were similar. This suggests that the lower E_c of VD-Gala than that of VV-Gala may result from the lower E_1 at the leaf scale. Similarly, Cohen and Naor (2002) demonstrated that lower sap flow in dwarf than vigorous apple trees resulted from the leaf hydraulic conductance because the LAI between treatments was similar. However, the E_c of VD-Fuji was higher than that of VV-Fuji. Both the higher E_1 and more favorable microclimate owing to lower LAI (Figure 6) and higher light interception efficiency (Yang et al., 2016) in VD-Fuji than VV-Fuji may contribute to the higher E_c of VD-Fuji than that of VV-Fuji. The virtual scenarios tested by switching interstock leaf distribution and function further dissected and verified that both VD leaf distribution and function enhanced E_c in 'Fuji'. Moreover, the VV trees could maintain higher g_s/g_{smax} under non-optimal environmental conditions, while not transpiring more water owing to their smaller g_{sl} compared with VD trees, irrespective of the cultivar. This led to higher WUE for VV trees and implied that water use was more conservative in vigorous interstock trees. This suggests that VV trees may be less sensitive to abiotic stress, possibly because of a stable leaf water status as suggested by previous studies (Liu et al., 2012; Bassett, 2013). In addition, 'Gala' leaf functions had a consistent effect on A_c , E_c and WUE_c , irrespective of the interstock or weather condition (Figure 8). However, the VD leaf functions had the opposite effect in 'Fuji' and 'Gala' (Figure 10). This suggests that cultivar leaf functions are independent of interstock, whereas interstock leaf functions depend on the cultivars.

3D architecture plays a crucial role in canopy carbon assimilation

Plant architecture has been reported to have a more profound effect on canopy photosynthesis at an early stage than at a stage with fully developed leaves in rice (Burgess et al., 2017). The simulations used steady-state leaf functions (such as g_{sl} , V_{cmax} and J_{max}) which are highly heterogeneous both temporally and spatially (Higgs and Jones, 1990; Ngao et al., 2017). In particular, the photosynthesis activity in leaves is higher at the beginning of the growing season (Greer, 2014). This could cause the photosynthesis activity in the canopy to be underestimated in the present work. However, the fully developed canopy, at which stage we measured leaf functions and architecture, was adequate to reveal differences among interstocks and cultivars.

In the reference scenario (S0), despite lower leaf-scale photosynthetic capacity in VD trees, A_c and WUE_c for 'Fuji' were significantly improved at the canopy scale in VD trees under both sunny and cloudy conditions, as well as for VD-Gala under cloudy conditions, when compared with the corresponding VV trees (Figure 9). It is likely that 3D architecture is responsible for higher A_c in VD trees through improved within-canopy light interception and micro-climate, which depend on weather conditions. In a previous study, we discovered that VD trees have a more even 3D leaf

distribution, which leads to better light interception and deeper light penetration into the canopy vertically and horizontally than VV trees in both 'Fuji' and 'Gala' (Yang et al., 2016). Solar radiation is composed of a diffuse and a direct component; the fraction of diffuse light is higher on cloudy days than sunny days. Moreover, the light environment in VD trees for 'Fuji' is significantly improved for both diffuse and direct light and is only significantly improved for 'Gala' in VD trees for diffuse light compared with the corresponding VV trees (Yang et al., 2016; Yang et al., 2017). Thus, we consider that the more even 3D leaf distribution in VD trees led to more leaves receiving greater light and that this higher light interception had a positive effect on leaf N_a (Figure 4), as suggested by the 'optimization theory' (Hirose and Werger, 1987). Therefore, the micro-climate around leaves (Woods et al., 2018) could be favorable and stimulate canopy photosynthetic potential in VD trees for 'Fuji' and 'Gala' under cloudy conditions.

Between interstocks, the leaf distribution of VD is more efficient than that of VV in improving A_c and WUE_c and similarly, the leaf distribution of 'Gala' is more efficient in improving A_c and WUE_c than 'Fuji' between cultivars owing to the reduced lower leaf clustering and within-tree self-shading (Yang et al., 2016). Thus, the relative frequency of leaves that are poorly illuminated is higher in VV than in VD and in 'Fuji' than in 'Gala', which results in higher dark respiration for maintenance. Furthermore, the positive effect of VD or 'Gala' leaf distribution on A_c and WUE_c was dissected and conformed by conducting a virtual scenario analysis (Figures 9, 10). This is consistent with previous studies in which a LAI above the optimal value was shown to lead to decreased A_c (Anten et al., 1995; Song et al., 2020).

An additional point thing to note is that under cloudy conditions, the leaf distribution of VD and 'Gala', as well as the leaf function of 'Gala', were more efficient than under sunny conditions. However, diffuse light interception efficiency improved under the leaf distribution of VD and Gala more than direct (Yang et al., 2017). This could be because diffuse light generates a more homogeneous light distribution within the canopy than direct light and can avoid the light saturation constraint resulting from high light intensity (Gu et al., 2002) and allows plants to use diffuse light more efficiently than direct light (Urban et al., 2012; Li and Yang, 2015). In addition, changes in light components will alter the microclimate, such as air and soil temperature and VPD, and thereby directly or indirectly influence stomatal responses (Urban et al., 2012). However, further study is needed to disentangle the relative contributions among leaf nitrogen, photosynthetic parameters (e.g. V_{cmax} , J_{max} and R_d) and stomatal responses to environmental factors.

A tradeoff between WUE and yield is suspected, as increase in plant WUE_c generally has been shown to result in reduced yield (Bassett, 2013). In the present study, the synchronous improvement of A_c and WUE_c indicated that selecting appropriate rootstock \times scion combinations could suppress this tradeoff. Moreover, several genetic markers have been identified for dwarfing rootstocks (Foster et al., 2015) and also for tree architecture, light interception, and proxies of leaf stomatal conductance and transpiration (Virlet et al., 2015; Coupel-Ledru et al., 2022). This suggests potential genetic improvement of canopy performances through modification of both tree architecture and leaf functions could be considered.

Conclusion

We showed that a dwarf interstock induced higher g_{sl} and transpiration in ‘Fuji’, and similar g_{sl} in dwarfed ‘Gala’ compared with those induced by a vigorous interstock. Dwarf interstock trees showed significantly lower leaf photosynthesis rate and WUE than vigorous trees. Canopy-scale simulations showed that lower leaf photosynthetic capacities and WUE were significantly improved in dwarf interstock trees compared with those of vigorous interstock trees. Switching scenarios highlighted that ‘Gala’ leaf functions and distribution and dwarf interstock leaf distributions enhanced canopy photosynthesis and WUE simultaneously, irrespective of weather conditions. This modeling approach paves the way to further optimize canopy photosynthetic capacity and WUE simultaneously through horticultural practices (e.g., rootstock and canopy management) that focus on both tree architecture and leaf functions.

Data availability statement

The datasets presented in this study can be found in online repositories. The names of the repository/repositories and accession number(s) can be found below: <http://doi.org/10.5281/zenodo.4049858>.

Author contributions

WY, XZ and DZ planned and designed the research. WY, XC and XZ performed experiments and conducted fieldwork. MS tested the model and provided related code. WY, XZ and EC implemented the models, analyzed the data, and wrote the manuscript. WY, XZ, EC, and MT reviewed and edited the manuscript. All authors contributed to the article and approved the submitted version.

References

- Aguirre, P. B., Al-Hinai, Y. K., Roper, T. R., and Krueger, A. R. (2001). Apple tree rootstock and fertilizer application timing affect nitrogen uptake. *Hortscience* 36, 1202–1205. doi: 10.21273/HORTSCI.36.7.1202
- Albacete, A., Martínez-Andújar, C., Martínez-Pérez, A., Thompson, A. J., Dodd, I. C., and Pérez-Alfocea, F. (2015). Unravelling rootstock × scion interactions to improve food security. *J. Exp. Bot.* 66, 2211–2226. doi: 10.1093/jxb/erv027
- An, H., Luo, F., Wu, T., Wang, Y., Xu, X., Zhang, X., et al. (2017). Effect of rootstocks or interstems on dry matter allocation in apple. *Eur. J. Hort. Sci.* 82, 225–231. doi: 10.17660/eJHS.2017/82.5.1
- Anten, N. P., Schieving, F., Medina, E., Werger, M., and Schuffelen, P. (1995). Optimal leaf area indices in C3 and C4 mono- and dicotyledonous species at low and high nitrogen availability. *Physiol. Plant* 95, 541–550. doi: 10.1111/j.1399-3054.1995.tb05520.x
- Barden, J. A., and Ferree, D. C. (1979). Rootstock does not affect net photosynthesis, dark respiration, specific leaf weight, and transpiration of apple leaves. *J. Am. Soc. Hort. Sci.* 104, 526–528. doi: 10.21273/JASHS.104.4.526
- Baron, D., Esteves Amaro, A. C., Pina, A., and Ferreira, G. (2019). An overview of grafting re-establishment in woody fruit species. *Sci. Hort.* 243, 84–91. doi: 10.1016/j.scienta.2018.08.012
- Bassett, C. L. (2013). “Water use and drought response in cultivated and wild apples,” in *Abiotic stress-plant responses applications in agriculture*. Eds. V. Kouroush and L. Charles. (Croatia: InTech), 249–275.
- Bauerle, W. L., Bowden, J. D., and Wang, G. G. (2007). The influence of temperature on within-canopy acclimation and variation in leaf photosynthesis: spatial acclimation to microclimate gradients among climatically divergent *Acer rubrum* l. genotypes. *J. Exp. Bot.* 58, 3285–3298. doi: 10.1093/jxb/erm177
- Bindi, M., Miglietta, F., and Zipoli, G. (1992). Different methods for separating diffuse and direct components of solar radiation and their application in crop growth models. *Climate Res.* 2, 47–54. doi: 10.3354/cr002047
- Blum, A. (2005). Drought resistance, water-use efficiency, and yield potential—are they compatible, dissonant, or mutually exclusive? *Crop Pasture Sci.* 56, 1159–1168. doi: 10.1071/AR05069
- Brutsaert, W. (1975). On a derivable formula for long-wave radiation from clear skies. *Water Resour. Res.* 11, 742–744. doi: 10.1029/WR011i005p00742
- Burgess, A. J., Retkute, R., Herman, T., and Murchie, E. H. (2017). Exploring relationships between canopy architecture, light distribution, and photosynthesis in contrasting rice genotypes using 3D canopy reconstruction. *Front. Plant Sci.* 8, 734. doi: 10.3389/fpls.2017.00734

Funding

This work was supported by the National Natural Science Foundation of China (31860527), Starting research fund from Shihezi University (RCSX201726).

Acknowledgments

We thank Jérôme Ngao for assistance in RATP simulation and Jean Luc Regnard for his assistance on calculation of stomatal conductance.

Conflict of interest

The authors declare that the research was conducted in the absence of any commercial or financial relationships that could be construed as a potential conflict of interest.

Publisher’s note

All claims expressed in this article are solely those of the authors and do not necessarily represent those of their affiliated organizations, or those of the publisher, the editors and the reviewers. Any product that may be evaluated in this article, or claim that may be made by its manufacturer, is not guaranteed or endorsed by the publisher.

Supplementary material

The Supplementary Material for this article can be found online at: <https://www.frontiersin.org/articles/10.3389/fpls.2023.1117051/full#supplementary-material>

- Chen, T.-W., Henke, M., De Visser, P. H. B., Buck-Sorlin, G., Wiechers, D., Kahlen, K., et al. (2014). What is the most prominent factor limiting photosynthesis in different layers of a greenhouse cucumber canopy? *Ann. Bot.* 114, 677–688. doi: 10.1093/aob/mcu100
- Cheng, L. L., and Fuchigami, L. H. (2000). Rubisco activation state decreases with increasing nitrogen content in apple leaves. *J. Exp. Bot.* 51, 1687–1694. doi: 10.1093/jxb/51.1351.1687
- Clearwater, M. J., Lowe, R. G., Hofstee, B. J., Barclay, C., Mandemaker, A. J., and Blattmann, P. (2004). Hydraulic conductance and rootstock effects in grafted vines of kiwifruit. *J. Exp. Bot.* 55, 1371–1382. doi: 10.1093/jxb/erh137
- Cohen, S., and Naor, A. (2002). The effect of three rootstocks on water use, canopy conductance and hydraulic parameters of apple trees and predicting canopy from hydraulic conductance. *Plant Cell Environ.* 25, 17–28. doi: 10.1046/j.1365-3040.2002.00795.x
- Cohen, S., Naor, A., Bennink, J., Grava, A., and Tyree, M. (2007). Hydraulic resistance components of mature apple trees on rootstocks of different vigours. *J. Exp. Bot.* 58, 4213–4224. doi: 10.1093/jxb/erm281
- Condon, A. G., Richards, R., Rebetzke, G., and Farquhar, G. (2004). Breeding for high water-use efficiency. *J. Exp. Bot.* 55, 2447–2460. doi: 10.1093/jxb/erh277
- Costes, E., and Garcia-Villanueva, E. (2007). Clarifying the effects of dwarfing rootstock on vegetative and reproductive growth during tree development: A study on apple trees. *Ann. Bot.* 100, 347–357. doi: 10.1093/aob/mcm114
- Costes, E., Lauri, P.É., and Regnard, J. (2006). Analyzing fruit tree architecture: Implications for tree management and fruit production. *Hortic. Rev.* 32, 1–61. doi: 10.1002/9780470767986.ch1
- Costes, E., Smith, C., Renton, M., Guédon, Y., Prusinkiewicz, P., and Godin, C. (2008). MAppleT: Simulation of apple tree development using mixed stochastic and biomechanical models. *Funct. Plant Biol.* 35, 936–950. doi: 10.1071/FP08081
- Coupeledru, A., Pallas, B., Delalande, M., Segura, V., Guitton, B., Muranty, H., et al. (2022). Tree architecture, light interception and water-use related traits are controlled by different genomic regions in an apple tree core collection. *New Phytol.* 234, 209–226. doi: 10.1111/nph.17960
- Development Core Team, R. (2020). *R: A language and environment for statistical computing*. 3.6.0 (Vienna, Austria: R Foundation for Statistical Computing).
- Di Vaio, C., Cirillo, C., Buccheri, M., and Limongelli, F. (2009). Effect of interstock (M. 9 and m. 27) on vegetative growth and yield of apple trees (cv “Annurca”). *Sci. Hortic.* 119, 270–274. doi: 10.1016/j.scienta.2008.08.019
- Donès, N., Adam, B., and Sinoquet, H. (2006). *PiafDigit—software to drive a Polhemus Fastrak 3 SPACE 3D digitiser and for the acquisition of plant architecture. Version 1.1*. Clermont-Ferrand: UMR PIAF INRA-UBP.
- Dragoni, D., Lakso, A. N., and Piccioni, R. M. (2004). Transpiration of an apple orchard in a cool humid climate: Measurement and modeling. *Acta Hortic.* 664, 175–180. doi: 10.17660/ActaHortic.2004.664.19
- Evans, J. R. (1989). Photosynthesis and nitrogen relationships in leaves of C3 plants. *Oecologia* 78, 9–19. doi: 10.1007/BF00377192
- Fallahi, E., Colt, W. M., Fallahi, B., and Chun, I.-J. (2002). The importance of apple rootstocks on tree growth, yield, fruit quality, leaf nutrition, and photosynthesis with an emphasis on ‘Fuji’. *HortTechnology* 12, 38–44. doi: 10.21273/HORTTECH.12.1.38
- Farque, L., Sinoquet, H., and Colin, F. (2001). Canopy structure and light interception in quercus petraea seedlings in relation to light regime and plant density. *Tree Physiol.* 21, 1257–1267. doi: 10.1093/treephys/21.17.1257
- Farquhar, G. D., von Caemmerer, S. V., and Berry, J. A. (1980). A biochemical model of photosynthetic CO₂ assimilation in leaves of C3 species. *Planta* 149, 78–90. doi: 10.1007/BF00386231
- Fazio, G., Robinson, T. L., and Aldwinckle, H. S. (2015). The Geneva apple rootstock breeding program. *Plant Breed.* 39, 379–424.
- Foster, T. M., Celton, J.-M., Chagné, D., Tustin, D. S., and Gardiner, S. E. (2015). Two quantitative trait loci, *Dw1* and *Dw2*, are primarily responsible for rootstock-induced dwarfing in apple. *Hortic. Res.* 2, 15001. doi: 10.1038/hortres.2015.1
- Foster, T. M., Mcatee, P. A., Waite, C. N., Boldingh, H. L., and Mcghee, T. K. (2017). Apple dwarfing rootstocks exhibit an imbalance in carbohydrate allocation and reduced cell growth and metabolism. *Hortic. Res.* 4, 17009. doi: 10.1038/hortres.2017.9
- Foster, T., Van Hooijdonk, B., Friend, A., Seleznyova, A., and McLachlan, A. (2016). Apple rootstock-induced dwarfing is strongly influenced by growing environment. *J. Hortic.* 3, 1000180. doi: 10.4172/2376-0354.1000180
- Fullana-Pericàs, M., Conesa, M. À., Pérez-Alfoceab, F., and Galmés, J. (2020). The influence of grafting on crops’ photosynthetic performance. *Plant Sci.* 295, 110250. doi: 10.1016/j.plantsci.2019.110250
- Génard, M., Baret, F., and Simon, D. (2000). A 3D peach canopy model used to evaluate the effect of tree architecture and density on photosynthesis at a range of scales. *Ecol. Model.* 128, 197–209. doi: 10.1016/S0304-3800(99)00232-X
- Gonçalves, B., Moutinho-Pereira, J., Santos, A., Silva, A. P., Bacelar, E., Correia, C., et al. (2006). Scion–rootstock interaction affects the physiology and fruit quality of sweet cherry. *Tree Physiol.* 26, 93–104. doi: 10.1093/treephys/26.1.93
- Greer, D. H. (2014). Seasonal changes in the photosynthetic response to CO₂ and temperature in apple (*Malus domestica* cv. ‘Red gala’) leaves during a growing season with a high temperature event. *Funct. Plant Biol.* 42, 309–324. doi: 10.1071/FP14208
- Greer, D. (2019). Limitations to photosynthesis of leaves of apple (*Malus domestica*) trees across the growing season prior to and after harvest. *Photosynthetica* 57, 483–490. doi: 10.32615/ps.2019.063
- Gu, L., Baldocchi, D., Verma, S. B., Black, T., Vesala, T., Falge, E. M., et al. (2002). Advantages of diffuse radiation for terrestrial ecosystem productivity. *J. Geophys. Res. Atmos.* 107, 2–23. doi: 10.1029/2001JD001242
- Han, Q., Guo, Q., Korpelainen, H., Niinemets, Ü., and Li, C. (2019). Rootstock determines the drought resistance of poplar grafting combinations. *Tree Physiol.* 39, 1855–1866. doi: 10.1093/treephys/tpz102
- Harley, P. C., Thomas, R. B., Reynolds, J. F., and Strain, B. R. (1992). Modelling photosynthesis of cotton grown in elevated CO₂. *Plant Cell Environ.* 15, 271–282. doi: 10.1111/j.1365-3040.1992.tb00974.x
- Higgs, K., and Jones, H. (1990). Response of apple rootstocks to irrigation in south-east England. *J. Hortic. Sci.* 65, 129–141. doi: 10.1080/00221589.1990.11516039
- Hikosaka, K. (2003). A model of dynamics of leaves and nitrogen in a plant canopy: an integration of canopy photosynthesis, leaf life span, and nitrogen use efficiency. *Am. Nat.* 162, 149–164. doi: 10.1086/376576
- Hirose, T., and Werger, M. (1987). Maximizing daily canopy photosynthesis with respect to the leaf nitrogen allocation pattern in the canopy. *Oecologia* 72, 520–526. doi: 10.1007/BF00378977
- Jarvis, P. (1976). The interpretation of the variations in leaf water potential and stomatal conductance found in canopies in the field. *Philos. Trans. R. Soc. B: Biol. Sci.* 273, 593–610. doi: 10.1098/rstb.1976.0035
- Jia, T. (1995). Dwarfing rootstock effect on leaf anatomical structure and photosynthesis. *J. Beijing Univ. Agric.* 2, 23–28.
- Lauri, P. E., Téroouanne, E., Lespinasse, J. M., Regnard, J. L., and Kelner, J. J. (1995). Genotypic differences in the axillary bud growth and fruiting pattern of apple fruiting branches over several years—an approach to regulation of fruit bearing. *Sci. Hortic.* 64, 265–281. doi: 10.1016/0304-4238(95)00836-5
- Le Roux, X., Grand, S., Dreyer, E., and Daudet, F. A. (1999). Parameterization and testing of a biochemically based photosynthesis model for walnut (*Juglans regia*) trees and seedlings. *Tree Physiol.* 19, 481–492. doi: 10.1093/treephys/19.8.481
- Le Roux, X., Walcroft, A., Daudet, F., Sinoquet, H., Chaves, M., Rodrigues, A., et al. (2001). Photosynthetic light acclimation in peach leaves: Importance of changes in mass: area ratio, nitrogen concentration, and leaf nitrogen partitioning. *Tree Physiol.* 21, 377–386. doi: 10.1093/treephys/21.6.377
- Li, M.-F., Tang, X.-P., Wu, W., and Liu, H.-B. (2013). General models for estimating daily global solar radiation for different solar radiation zones in mainland China. *Energy Convers. Manage.* 70, 139–148. doi: 10.1016/j.enconman.2013.03.004
- Li, T., and Yang, Q. (2015). Advantages of diffuse light for horticultural production and perspectives for further research. *Front. Plant Sci.* 6, 704. doi: 10.3389/fpls.2015.00704
- Liu, B. H., Cheng, L., Liang, D., Zou, Y. J., and Ma, F. W. (2012). Growth, gas exchange, water-use efficiency, and carbon isotope composition of ‘Gala’ apple trees grafted onto 9 wild Chinese rootstocks in response to drought stress. *Photosynthetica* 50, 401–410. doi: 10.1007/s11099-012-0048-0
- Massonnet, C., Costes, E., Rambal, S., Dreyer, E., and Regnard, J. L. (2007). Stomatal regulation of photosynthesis in apple leaves: Evidence for different water-use strategies between two cultivars. *Ann. Bot.* 100, 1347–1356. doi: 10.1093/aob/mcm222
- Massonnet, C., Regnard, J., Lauri, P.É., Costes, E., and Sinoquet, H. (2008). Contributions of foliage distribution and leaf functions to light interception, transpiration and photosynthetic capacities in two apple cultivars at branch and tree scales. *Tree Physiol.* 28, 665. doi: 10.1093/treephys/28.5.665
- Migicovsky, Z., Harris, Z. N., Klein, L. L., Li, M., Mcdermaid, A., Chitwood, D. H., et al. (2019). Rootstock effects on scion phenotypes in a ‘Chambourcin’ experimental vineyard. *Hortic. Res.* 6, 64. doi: 10.1038/s41438-019-0146-2
- Minas, I. S., Tanou, G., and Molassiotis, A. (2018). Environmental and orchard bases of peach fruit quality. *Sci. Hortic.* 235, 307–322. doi: 10.1016/j.scienta.2018.01.028
- Monteith, J. L. (1977). Climate and the efficiency of crop production in Britain. *Philos. Trans. R. Soc. Lond. B Biol. Sci.* 281, 277–294. doi: 10.1098/rstb.1977.0140
- Ngao, J., Adam, B., and Saudreau, M. (2017). Intra-crown spatial variability of leaf temperature and stomatal conductance enhanced by drought in apple tree as assessed by the RATP model. *Agr. For. Meteorol.* 237, 340–354. doi: 10.1016/j.agrformet.2017.02.036
- Niinemets, Ü., and Tenhunen, J. D. (1997). A model separating leaf structural and physiological effects on carbon gain along light gradients for the shade-tolerant species *Acer saccharum*. *Plant Cell Environ.* 20, 845–866. doi: 10.1046/j.1365-3040.1997.d01133.x
- Niinemets, Ü., Keenan, T. F., and Hallik, L. (2015). A worldwide analysis of within-canopy variations in leaf structural, chemical and physiological traits across plant functional types. *New Phytol.* 205, 973–993. doi: 10.1111/nph.13096
- Nolan, W. G., and Smillie, R. M. (1976). Multi-temperature effects on hill reaction activity of barley chloroplasts. *Biochim. Biophys. Acta - Bioenerg.* 440, 461–475. doi: 10.1016/0005-2728(76)90034-7
- Olien, W., and Lakso, A. (1986). Effect of rootstock on apple (*Malus domestica*) tree water relations. *Physiol. Plant* 67, 421–430. doi: 10.1111/j.1399-3054.1986.tb05757.x
- Pallas, B., Martinez, S., Simler, O., Carrie, E., Costes, E., and Boudon, F. (2020). Assessing T-LiDAR technology for high throughput phenotyping apple tree topological

- and architectural traits. *Acta Hort.* 1281, 625–632. doi: 10.17660/ActaHortic.2020.1281.82
- Peccoux, A., Loveys, B., Zhu, J., Gambetta, G. A., Delrot, S., Vivin, P., et al. (2018). Dissecting the rootstock control of scion transpiration using model-assisted analyses in grapevine. *Tree Physiol.* 38, 1026–1040. doi: 10.1093/treephys/tpx153
- Picheny, V., Casadebaig, P., Trépos, R., Faivre, R., Da Silva, D., Vincourt, P., et al. (2017). Using numerical plant models and phenotypic correlation space to design achievable ideotypes. *Plant Cell Environ.* 40, 1926–1939. doi: 10.1111/pce.13001
- Poorter, H., Niinemets, Ü., Ntagkas, N., Siebenkäs, A., Mäenpää, M., Matsubara, S., et al. (2019). A meta-analysis of plant responses to light intensity for 70 traits ranging from molecules to whole plant performance. *New Phytol.* 223, 1073–1105. doi: 10.1111/nph.15754
- Pradal, C., Dufour-Kowalski, S., Boudon, F., Fournier, C., and Godin, C. (2008). OpenAlea: a visual programming and component-based software platform for plant modelling. *Funct. Plant Biol.* 35, 751–760. doi: 10.1071/FP08084
- Pratt, C. (1988). Apple flower and fruit: morphology and anatomy. *Hortic. Rev.* 10, 273–308. doi: 10.1002/9781118060834.ch8
- Preston, A. P. (1967). Apple rootstock studies: Fifteen years' results with some M.IX crosses. *J. Hort. Sci.* 42, 41–50. doi: 10.1080/00221589.1967.11514191
- Reyes, F., Pallas, B., Pradal, C., Vaggi, F., Zanotelli, D., Tagliavini, M., et al. (2018). MuSCA: a multi-scale model to explore carbon allocation in plants. *Ann. Bot.* 126, 571–585. doi: 10.1093/aob/mcz122
- Samuolienė, G., Viškelienė, A., Sirtautas, R., and Kviklys, D. (2016). Relationships between apple tree rootstock, crop-load, plant nutritional status and yield. *Sci. Hort.* 211, 167–173. doi: 10.1016/j.scienta.2016.08.027
- Schedter, I., Elfving, D., and Proctor, J. (1991). Apple tree canopy development and photosynthesis as affected by rootstock. *Canad. J. Bot.* 69, 295–300. doi: 10.1139/b91-039
- Seleznyova, A., Thorp, T., White, M., Tustin, S., and Costes, E. (2003). Application of architectural analysis and AMAPmod methodology to study dwarfing phenomenon: the branch structure of 'Royal gala' apple grafted on dwarfing and non-dwarfing rootstock/interstock combinations. *Ann. Bot.* 91, 665–672. doi: 10.1093/aob/mcg072
- Sharma, R., Dubey, A., Awasthi, O., and Kaur, C. (2016). Growth, yield, fruit quality and leaf nutrient status of grapefruit (*Citrus paradisi* macf.): variation from rootstocks. *Sci. Hort.* 210, 41–48. doi: 10.1016/j.scienta.2016.07.013
- Sinoquet, H., Le Roux, X., Adam, B., Ameglio, T., and Daudet, F. A. (2001). RATP: a model for simulating the spatial distribution of radiation absorption, transpiration and photosynthesis within canopies: application to an isolated tree crown. *Plant Cell Environ.* 24, 395–406. doi: 10.1046/j.1365-3040.2001.00694.x
- Solari, L. I., Johnson, S., and Dejong, T. M. (2006). Hydraulic conductance characteristics of peach (*Prunus persica*) trees on different rootstocks are related to biomass production and distribution. *Tree Physiol.* 26, 1343–1350. doi: 10.1093/treephys/26.10.1343
- Song, Q., Srinivasan, V., Long, S. P., and Zhu, X.-G. (2020). Decomposition analysis on soybean productivity increase under elevated CO₂ using 3-d canopy model reveals synergistic effects of CO₂ and light in photosynthesis. *Ann. Bot.* 126, 601–614. doi: 10.1093/aob/mcz163
- Sotiropoulos, T.E. (2008). Performance of the apple (*Malus domestica* borkh.) cultivar imperial double red delicious grafted on five rootstocks. *Hortic. Sci.* 35, 7–11. doi: 10.17221/645-HORTSCI
- Spitters, C. J. T., Toussaint, H., and Goudriaan, J. (1986). Separating the diffuse and direct component of global radiation and its implications for modeling canopy photosynthesis part i. components of incoming radiation. *Agr. For. Meteorol.* 38, 217–229. doi: 10.1016/0168-1923(86)90060-2
- Strong, D., and Azarenko, A. N. (2000). Relationship between trunk cross-sectional area, harvest index, total tree dry weight and yield components of 'Starkspur supreme delicious' apple trees. *J. Am. Pomol. Soc.* 54, 22–27.
- Tombesi, S., Johnson, R. S., Day, K. R., and Dejong, T. M. (2009). Relationships between xylem vessel characteristics, calculated axial hydraulic conductance and size-controlling capacity of peach rootstocks. *Ann. Bot.* 105, 327–331. doi: 10.1093/aob/mcp281
- Tworkoski, T., and Fazio, G. (2015). Effects of size-controlling apple rootstocks on growth, abscisic acid, and hydraulic conductivity of scion of different vigor. *Int. J. Fruit Sci.* 15, 369–381. doi: 10.1080/15538362.2015.1009973
- Tworkoski, T., and Miller, S. (2007). Rootstock effect on growth of apple scions with different growth habits. *Sci. Hort.* 111, 335–343. doi: 10.1016/j.scienta.2006.10.034
- Urban, O., Klem, K., Ač, A., Havránková, K., Holišová, P., Navrátil, M., et al. (2012). Impact of clear and cloudy sky conditions on the vertical distribution of photosynthetic CO₂ uptake within a spruce canopy. *Funct. Ecol.* 26, 46–55. doi: 10.1111/j.1365-2435.2011.01934.x
- Van Hooijdonk, B., Warton, D., and Warrington, I. (2011). Rootstocks modify scion architecture, endogenous hormones and root growth of newly grafted 'Royal gala' apple trees. *J. Am. Soc. Hort. Sci.* 136, 93–102. doi: 10.21273/JASHS.136.2.93
- Virlet, N., Costes, E., Martinez, S., Kelner, J. J., and Regnard, J. L. (2015). Multispectral airborne imagery in the field reveals genetic determinisms of morphological and transpiration traits of an apple tree hybrid population in response to water deficit. *J. Exp. Bot.* 66, 5453–5465. doi: 10.1093/jxb/erv355
- Walcroft, A., Le Roux, X., Diaz-Espejo, A., Dones, N., and Sinoquet, H. (2002). Effects of crown development on leaf irradiance, leaf morphology and photosynthetic capacity in a peach tree. *Tree Physiol.* 22, 929–938. doi: 10.1093/treephys/22.13.929
- Walker, A. P., Beckerman, A. P., Gu, L., Kattge, J., Cernusak, L. A., Domingues, T. F., et al. (2014). The relationship of leaf photosynthetic traits— V_{cmax} and J_{max} —to leaf nitrogen, leaf phosphorus, and specific leaf area: a meta-analysis and modeling study. *Ecol. Evol.* 4, 3218–3235. doi: 10.1002/ece3.1173
- Warschefskey, E. J., Klein, L. L., Frank, M. H., Chitwood, D. H., Londo, J. P., Von Wettberg, E. J., et al. (2016). Rootstocks: diversity, domestication, and impacts on shoot phenotypes. *Trends Plant Sci.* 21, 418–437. doi: 10.1016/j.tplants.2015.11.008
- Webster, A. D. (1995). Rootstock and interstock effects on deciduous fruit tree vigour, precocity, and yield productivity. *N. Z. J. Crop Hort. Sci.* 23, 373–382. doi: 10.1080/01140671.1995.9513913
- Woods, H. A., Saudreau, M., and Pincebourde, S. (2018). Structure is more important than physiology for estimating intracanalopy distributions of leaf temperatures. *Ecol. Evol.* 8, 5206–5218. doi: 10.1002/ece3.4046
- Wünsche, J. N., Greer, D. H., Laing, W. A., and Palmer, J. W. (2005). Physiological and biochemical leaf and tree responses to crop load in apple. *Tree Physiol.* 25, 1253–1263. doi: 10.1093/treephys/25.10.1253
- Xu, H., and Ediger, D. (2021). Rootstocks with different vigor influenced scion–water relations and stress responses in Ambrosia™ apple trees (*Malus domestica* var. ambrosia). *Plants* 10, 614. doi: 10.3390/plants10040614
- Yang, W., Chen, X., Saudreau, M., Zhang, X., Zhang, M., Liu, H., et al. (2016). Canopy structure and light interception partitioning among shoots estimated from virtual trees: comparison between apple cultivars grown on different interstocks on the Chinese loess plateau. *Trees - Struct. Funct.* 30, 1723–1734. doi: 10.1007/s00468-016-1403-8
- Yang, W., Chen, X., Zhang, M., Gao, C., Liu, H., Saudreau, M., et al. (2017). Light interception characteristics estimated from three-dimensional virtual plants for two apple cultivars and influenced by combinations of rootstocks and tree architecture in loess plateau of China. *Acta Hort.* 1160, 245–252. doi: 10.17660/ActaHortic.2017.1160.36
- Yang, W., Ma, X., Ma, D., Shi, J., Hussain, S., Han, M., et al. (2021). Modeling canopy photosynthesis and light interception partitioning among shoots in bi-axis and single-axis apple trees (*Malus domestica* borkh.). *Trees - Struct. Funct.* 35, 845–861. doi: 10.1007/s00468-021-02085-z
- Yang, W., Zhang, X., Saudreau, M., Zhang, D., Costes, E., and Han, M. (2019). Photosynthetic capacity in 'Fuji' apple trees influenced by interstocks at leaf and canopy scale. *Acta Hort.* 1261, 77–84. doi: 10.17660/ActaHortic.2019.1261.14
- Zhang, Y., Henke, M., Li, Y., Xu, D., Liu, A., Liu, X., et al. (2022b). Analyzing the impact of greenhouse planting strategy and plant architecture on tomato plant physiology and estimated dry matter. *Front. Plant Sci.* 13, 828252. doi: 10.3389/fpls.2022.828252
- Zhang, X., Li, S., Tang, T., Liu, Y., Mobeen Tahir, M., Wang, C., et al. (2022a). Comparison of morphological, physiological, and related-gene expression responses to saline-alkali stress in eight apple rootstock genotypes. *Sci. Hort.* 306, 111455. doi: 10.1016/j.scienta.2022.111455
- Zhou, Y., Tian, X., Yao, J., Zhang, Z., Wang, Y., Zhang, X., et al. (2020). Morphological and photosynthetic responses differ among eight apple scion-rootstock combinations. *Sci. Hort.* 261, 108981. doi: 10.1016/j.scienta.2019.108981
- Zhu, J., Génard, M., Poni, S., Gambetta, G. A., Vivin, P., Vercambre, G., et al. (2019). Modelling grape growth in relation to whole-plant carbon and water fluxes. *J. Exp. Bot.* 70, 2505–2521. doi: 10.1093/jxb/ery367